Available online at www.sciencedirect.com
ScienceDirect
Inorganica Chimica Acta 361 (2008) 2210–2224
Inorganica Chimica Acta
www.elsevier.com/locate/ica

Delving into the complex picture of Ti(IV)–citrate speciation in aqueous media: Synthetic, structural, and electrochemical considerations in mononuclear Ti(IV) complexes containing variably deprotonated citrate ligands

Panagiotis Panagiotidis [a], Evangelos T. Kefalas [b], Catherine P. Raptopoulou [c], Aris Terzis [c], Thomas Mavromoustakos [d], Athanasios Salifoglou [a,*]

[a] *Laboratory of Inorganic Chemistry, Department of Chemical Engineering, Aristotle University of Thessaloniki, Thessaloniki 54124, Greece*
[b] *Department of Chemistry, University of Crete, Heraklion 71409, Greece*
[c] *Institute of Materials Science, NCSR "Demokritos", Aghia Paraskevi 15310, Attiki, Greece*
[d] *National Institute of Research, Athens 11635, Greece*

Received 3 August 2007; received in revised form 31 October 2007; accepted 8 November 2007
Available online 21 November 2007

Abstract

The aqueous reaction of $TiCl_4$ with citric acid at pH ~ 4 (KOH), led to the surprising isolation of a species assembly $K_3[Ti(C_6H_6O_7)_2(C_6H_5O_7)] \cdot K_4[Ti(C_6H_5O_7)_2(C_6H_6O_7)] \cdot 10H_2O$ (**1**). The same system at pH ~ 3 (neocuproine), led to the crystalline material $(C_{14}H_{13}N_2)_2[Ti(C_6H_6O_7)_3] \cdot 5H_2O$ (**2**), while at pH 5.0 (NaOH), afforded $Na_3[Ti(C_6H_6O_7)_2(C_6H_5O_7)] \cdot 9H_2O$ (**3**). Analytical, spectroscopic and structural characterization of **1**, **2** and **3** revealed their distinct nature exemplified by mononuclear complexes bearing variably deprotonated citrates bound to Ti(IV). Solid-state ^{13}C MAS NMR spectroscopy in concert with solution ^{13}C and ^{1}H NMR on **3** provided ample evidence for the existence of bound citrates of distinct coordination mode to the metal ion. Cyclic voltammetry defined the electrochemical signature of complex **2**, thereby projecting the physicochemical profile of the species formulated by the aforementioned properties. Comparison of cyclic voltammetric data on available discrete Ti(IV)–citrate species depicts the electrochemical profile and an $E_{1/2}$ value trend of the species in that binary system's aqueous speciation, further substantiating the redox behavior of mononuclear Ti(IV)–citrate species in a pH-sensitive fashion. Collectively, the well-defined discrete species in **1**–**3** reflect and corroborate a synthetically challenging yet complex pH-specific picture of the aqueous Ti(IV) chemistry with the physiological citric acid, and shed light on the pH-dependent speciation in the binary Ti(IV)–citrate system.

Keywords: Ti(IV)–citrate speciation; Mononuclear species; Aqueous complex synthesis; α-Hydroxycarboxylate ligands; Cyclic voltammetry

1. Introduction

Titanium, as a metal, has found numerous applications across the spectrum of metallurgical, biological, and medical sciences [1–6]. As a fairly light metal, it has been used as a component in industrial materials and alloys for prosthetic devices implanted to patients with orthopaedic problems or dysfunctions [7], in dental fillings [8,9], and others [10–12]. In the form of soluble Ti(III)–citrate, it has been used to promote redox support to enzymes being investigated for their mechanistic involvement in metallobiological processes, with nitrogenase [13] being a characteristic example.

In the context of biological processes, titanium comes in contact with biological tissues, thereby giving rise to chemical interactions with a variety of biological targets. As a result of such interactions, solubilization is imparted,

* Corresponding author. Tel.: +30 2310 996 179; fax: +30 2310 996 196.
E-mail address: salif@auth.gr (A. Salifoglou).

0020-1693/$ - see front matter © 2007 Elsevier B.V. All rights reserved.
doi:10.1016/j.ica.2007.11.015

affording soluble forms of the metal ion in its two predominant oxidation states Ti(III) and Ti(IV). Both high and low molecular mass ligands have the potential to interact with titanium. The arising complexes constitute potential partners in further interactions with molecular components in the intracellular or extracellular matrix, with all the known or unknown symptomatic toxic and/or non-toxic implications at the macroscopic clinical level. The importance of titanium interactions with molecular targets in the cellular milieu constitutes the essence of that metal's potential biological involvement, and such interactions have been the subject of numerous studies inquiring into their nature and implications at the clinical level [14–16].

In view of the fact that variable molecular mass ligands interact with titanium, emphasis was initially given by our lab to the study of low molecular mass physiological biomolecules with titanium(IV). Key to this thesis is the underlying aqueous speciation of Ti(IV) in the presence of physiological ligands promoting solubilization, which in turn begets bioavailability and supports cellular interactions. In an attempt to investigate and understand the aqueous chemistry of titanium(IV) in the presence of predominantly physiological ligands, citric acid was chosen to initiate relevant synthetic efforts. Citric acid, an α-hydroxycarboxylic acid, is plentiful in human plasma and capable of promoting metal ion binding, solubilization and ultimate absorption by various biological loci [17,18]. In view of the fact that structural information on relevant binary Ti(IV)–citrate [19] and ternary Ti(IV)-peroxo-citrate [20,21] systems are crucial in understanding the requisite aqueous interactions, we have launched synthetic efforts targeting the pH-dependent synthesis and physicochemical characterization of soluble binary complexes between Ti(IV) and the abundantly present citric acid in human plasma. Hence, we report herein on the synthesis, isolation, and characterization of binary Ti(IV)–citrate compounds exemplifying (a) the aqueous chemistry linked to the relevant structural speciation, (b) the diversity of species at a specific pH, (c) the complex yet potentially biologically relevant variable deprotonation state of citrate ligands bound to Ti(IV) centers, and (d) the arising pH-sensitive dependence of the redox behavior of known Ti(IV)–citrate structural variants in the context of that binary system's aqueous speciation.

2. Experimental

2.1. Materials and methods

All experiments were carried out in the open air. Nanopure quality water was used for all reactions. $TiCl_4$, anhydrous citric acid and citric acid monohydrate, potassium and sodium hydroxide, and neocuproine were purchased from Aldrich. Ammonia was supplied by Fluka. FT-Infrared measurements were taken on a Perkin Elmer 1760X FT-Infrared spectrometer. Elemental analyses were performed by a ThermoFinnigan Flash EA 1112 CHNS elemental analyzer. Specifically, the analyzer was used for the simultaneous determination of carbon, hydrogen, and nitrogen (%). The analyzer is based on the dynamic flash combustion of the sample (at 1800 °C) followed by reduction, trapping, complete GC separation and detection of the products. The instrument is (a) fully automated and controlled by PC via the Eager 300 dedicated software, and (b) capable of handling solid, liquid or gaseous substances.

2.1.1. Solid-state NMR

The high resolution solid-state ^{13}C Magic Angle Spinning (MAS) NMR spectra were measured at 100.63 MHz, on a Bruker MSL400 NMR spectrometer, capable of high power ^{1}H-decoupling. The spinning rate used for ^{1}H–^{13}C cross polarization and magic angle spinning experiments was 5 kHz at ambient temperature (25 °C). Each solid-state spectrum was a result of the accumulation of 200 scans. The recycle delay used was 4s, the 90° pulse was 5 μs, and the contact time was 1 ms. All solid-state spectra were referenced to adamantane, which showed two peaks at 26.5 and 37.6 ppm, respectively, and to the external reference of TMS.

2.1.2. Solution NMR

The samples for solution NMR studies were prepared by dissolving the crystalline complexes in D_2O, at concentrations in the range 0.02–0.10 M. NMR spectra were recorded on a Bruker AM360 (^{13}C) spectrometer. Chemical shifts (δ) are reported in ppm relative to an internal reference of TMS.

2.1.3. Cyclic voltammetry

Electrochemical measurements were carried out with a Uniscan Instruments Ltd. model PG580 potensiostat–galvanostat. The entire system was under computer control and supported by the appropriate computer software Ui Chem Version 1.08RD, running on Windows. The electrochemical cell used had platinum (disk) working and auxiliary (wire) electrodes. As reference electrode, a saturated calomel electrode (SCE) was used. The water used in the electrochemical measurements was of nanopure quality. KNO_3 was used as a supporting electrolyte. Normal concentrations used were 1–6 mM in electroanalyte and 0.1 M in supporting electrolyte. Purified argon was used to purge the solutions prior to the electrochemical measurements. Derived E values were converted to potentials vs. NHE prior to comparing them to literature values from cyclic voltammetric studies in the binary Ti(IV)–citrate system.

2.2. Preparation of $K_7[Ti(C_6H_6O_7)_2(C_6H_5O_7)] \cdot [Ti(C_6H_5O_7)_2(C_6H_6O_7)] \cdot 10H_2O$ (**1**)

A quantity of anhydrous citric acid (0.38 g, 2.0 mmol) was placed in a flask and dissolved in 2 mL of H_2O. To the clear solution, $TiCl_4$ (0.20 g, 1.0 mmol) was added

slowly and under continuous stirring. The resulting reaction mixture was allowed to stir overnight at room temperature. On the following day, aqueous potassium hydroxide solution (1:1 in water) was added slowly to adjust the pH to a final value of ~4.0. Then, the reaction flask was placed in the refrigerator. The addition of cold ethanol at 4 °C resulted after several days in the isolation of a colorless crystalline material. The product was isolated by filtration and dried in vacuo. The reaction affords the same crystalline material with comparable yields and a molar ratio Ti(IV): citric acid = 1:3 at pH 4.5. Yield: 0.39 g (44 %). *Anal.* Calc. for **1**, $K_3[Ti(C_6H_6O_7)_2(C_6H_5O_7)] \cdot K_4[Ti(C_6H_5O_7)_2(C_6H_6O_7)] \cdot 10H_2O$, ($C_{36}H_{53}K_7O_{52}Ti_2$): C, 25.60; H, 3.14; K, 16.22. Found: C, 25.68; H, 2.93; K, 16.38%.

2.3. Preparation of $(C_{14}H_{13}N_2)_2[Ti(C_6H_6O_7)_3] \cdot 5H_2O$ (2)

A quantity of anhydrous citric acid (0.19 g, 0.99 mmol) was placed in a flask and dissolved in 2 mL of H_2O. Subsequently, $TiCl_4$ (0.20 g, 1.0 mmol) was added slowly and under continuous stirring. Initially, the resulting reaction mixture was slightly cloudy, yet it was allowed to stir at room temperature overnight. Next day, 2,9-dimethyl-1,10-phenanthroline (neocuproine) (0.22 g, 1.0 mmol) was added slowly and under continuous stirring. An additional 2 mL of water was added and the resulting reaction mixture was stirred at room temperature overnight. On the following morning, the solution was slightly yellow and clear. The pH of the reaction mixture was 3. After a brief stay at 4 °C, the reaction flask was allowed to stand at room temperature for slow evaporation. A few days later, a colorless crystalline material was deposited at the bottom of the flask. The product was isolated by filtration and dried in vacuo. Yield: 0.45 g (38%). *Anal.* Calc. for $(C_{14}H_{13}N_2)_2[Ti(C_6H_6O_7)_3] \cdot 5H_2O$ (**2**), $C_{46}H_{54}N_4O_{26}Ti$: C, 48.99; H, 4.79; N, 4.97. Found: C, 48.89; H, 4.69; N, 4.79%.

2.4. Preparation of $Na_3[Ti(C_6H_6O_7)_2(C_6H_5O_7)] \cdot 9H_2O$ (3)

A quantity of citric acid monohydrate (0.66 g, 3.1 mmol) was placed in a flask and dissolved in 3 mL of H_2O. Subsequently, $TiCl_4$ (0.20 g, 1.0 mmol) was added slowly and under continuous stirring. Initially, the resulting reaction mixture was slightly cloudy, yet it was allowed to stir at room temperature overnight. On the following morning, the solution was clear. Next, a solution of sodium hydroxide (0.1 M) was added slowly and under continuous stirring. The pH of the reaction mixture was adjusted to 5. The addition of cold methanol at 4 °C resulted after a couple of months in the isolation of a colorless crystalline material. The colorless crystalline material was deposited at the bottom of the flask. The product was isolated by filtration and dried in vacuo. Yield: 0.48 g (54 %). *Anal.* Calc. for $Na_3[Ti(C_6H_6O_7)_2(C_6H_5O_7)] \cdot 9H_2O$ (**3**), $C_{18}H_{35}Na_3O_{30}$-Ti: C, 25.46; H, 4.13. Found: C, 25.67; H, 4.09%.

2.5. X-ray crystallographic determination

X-ray quality crystals of compounds **1**, **3** and **2** were grown from water–ethanol, water–methanol mixtures and slow evaporation, respectively. A single crystal, with dimensions $0.08 \times 0.15 \times 0.50$ mm (**1**), $0.20 \times 0.30 \times 0.50$ mm (**2**), and $0.50 \times 0.20 \times 0.08$ mm (**3**) was mounted on a Crystal Logic dual-goniometer diffractometer, using graphite monochromated Mo Kα radiation ($\lambda = 0.71073$ Å). Unit cell dimensions for **1**–**3** were determined and refined by using the angular settings of 25 automatically centered reflections in the range $11 < 2\theta < 23°$. Crystallographic details are given in Table 1. Intensity data were measured by using θ–2θ scans. Three standard reflections were monitored every 97 reflections, over the course of data collection at 298 K. They showed less than 3% variation and no decay. Lorentz and polarization corrections were applied by using Crystal Logic software. The structures of complexes **1**–**3** were solved by direct methods using SHELXS-86 [22]. Refinement was achieved by full-matrix least-squares techniques on F^2 with SHELXL-97 [23]. All non-H atoms in the structure of **1** were refined anisotropically. Ten water molecules of crystallization were found to be present in the lattice of **1**. All the H-atoms of the anion in **1** were located by difference maps and were refined isotropically. All non-H atoms in **2** were refined anisotropically, except for the fourth and the fifth lattice water molecules. The latter molecule was found to be disordered over two positions and it was refined isotropically with occupancy factors of total sum one (0.62 and 0.38, respectively). The terminal carboxylate group defined by C(6), O(6), and O(7) was found to be disordered and it was refined anisotropically over two positions, with occupancy factors of total sum one (0.59 and 0.41, respectively). The oxygen atoms O(26) and O(27) of the terminal carboxylate group, belonging to the third citrate ligand, were also found to be disordered and were refined anisotropically over two positions, with occupancy factors of total sum one (0.38 and 0.62, respectively). Thus, no hydrogen atoms for these terminal carboxylates were included in the refinement. All H-atoms of the citrate ligands (except for those of the protonated carboxylates that were located by difference maps and were refined isotropically) and the cations were introduced at calculated positions as riding on bonded atoms. The second cation and the strongly H-bonded water molecule (OW3) were found to be disordered over two positions and were refined anisotropically with occupancy factors of total sum one (0.72 and 0.28, respectively). Five lattice water molecules were found to be present in the lattice of **2**. No hydrogen atoms were found for the lattice water molecules. All non-H atoms in **3** were refined anisotropically. H-atoms of the citrate ligands were located by difference maps and were refined isotropically. Sodium ions Na(3) and Na(4) were found disordered around a twofold axis and a center of symmetry, respectively, and were refined anisotropically with an occupancy factor fixed at 0.50. Nine water molecules of crystallization

Table 1
Crystallographic data for compounds **1**, **2** and **3**

	1	**2**	**3**
Empirical formula	$C_{36}H_{53}K_7O_{52}Ti_2$	$C_{46}H_{54}N_4O_{26}Ti$	$C_{18}H_{35}Na_3O_{30}Ti$
Formula weight	1687.28	1126.83	848.33
Crystal system	triclinic	triclinic	monoclinic
Space group	$P\bar{1}$	$P\bar{1}$	$C2/c$
a (Å)	11.222(6)	13.91(1)	18.961(5)
b (Å)	16.669(9)	14.192(9)	10.955(3)
c (Å)	18.68(1)	16.13(1)	31.655(9)
α (°)	68.17(2)	65.68(2)	90.00
β (°)	84.6(2)	66.85(2)	97.430(10)
γ (°)	74.73(2)	86.93(2)	90.00
V (Å^3)	3128.3(3)	2646(3)	6520(3)
Z	2	2	8
ρ_{calc} (mg/m^3)	1.791	1.414	1.728
$F(000)$	1724	1176	3504
μ (mm^{-1})	0.844	0.253	0.419
Temperature (K)	298	298	298
$2\theta_{max}$ (°)	46	50	50
Reflections collected	9019	9957	5839
Independent reflections (R_{int})	8697 (0.0351)	9293 (0.0277)	5722 (0.0117)
Observed reflections [$I > 2\sigma(I)$]	7100	7350	4969
Data/restraints/parameters	8697/0/1046	9293/0/906	5722/0/591
Goodness-of-fit on F^2	1.057	1.064	1.034
Final R indices [$I > 2\sigma(I)$][d]	$R = 0.0437$	$R = 0.0647$	$R = 0.0571$
	$R_w = 0.1123$[a]	$R_w = 0.1875$[b]	$R_w = 0.1616$[c]
R indices for all data[d]	$R = 0.0569$	$R = 0.0812$	$R = 0.0650$
	$R_w = 0.1223$	$R_w = 0.2049$	$R_w = 0.1709$

$R = \frac{\sum ||F_o| - |F_c||}{\sum (|F_o|)}$, $R_w = \sqrt{\sum [w(F_o^2 - F_c^2)^2] / \sum [w(F_o^2)^2]}$.

[a] For 7100 reflections with $(I) > 2\sigma(I)$.

[b] For 7350 reflections with $(I) > 2\sigma(I)$.

[c] For 4969 reflections with $(I) > 2\sigma(I)$.

[d] R values are based on F values, R_w values are based on F^2.

were refined anisotropically, with some of their H-atoms having been located by difference maps and refined isotropically. The remaining H-atoms were not included in the refinement. One of the water molecules of crystallization was found to be disordered over three positions and was refined anisotropically with occupancy factors fixed at 0.40, 0.35 and 0.25, respectively.

3. Results

3.1. Syntheses

The expedient synthesis of complex **1** was achieved by reacting $TiCl_4$ and citric acid, in water, with a molar ratio of 1:2. The addition of aqueous potassium hydroxide was critical in that KOH not only raised the pH of the solution to ~4, but also provided the necessary counter ions for the subsequently derived anionic complexes. The resulting colorless reaction mixture was treated with ethanol at 4 °C and afforded a colorless crystalline material in a few days. Attempts to run the reaction with a Ti(IV): citric acid molar ratio 1:3 at pH 4.5 were equally successful, and under similar reaction conditions led to the isolation of the same crystalline product. Elemental analysis on the isolated crystalline material suggested the formulation $3K_3[Ti(C_6H_6O_7)_2(C_6H_5O_7)] \cdot K_4[Ti(C_6H_5O_7)_2(C_6H_6O_7)] \cdot 10H_2O$ (**1**). In a similar reaction, $TiCl_4$ and citric acid (molar ratio 1:1) reacted in water at pH ~ 3, with neocuproine acting as a base and generating the thus produced counter ions in the crystalline product. The latter emerged through slow evaporation of the reaction mixture. The molecular formulation of the product based on elemental analysis was $(C_{14}H_{13}N_2)_2[Ti(C_6H_6\ O_7)_3] \cdot 5H_2O$ (**2**). When the same reaction was run in the presence of NaOH at pH 5, it led to the isolation of yet another crystalline material $Na_3[Ti(C_6H_6O_7)_2(C_6H_5O_7)] \cdot 9H_2O$ (**3**). The overall stoichiometric reactions for complexes **1**, **2** and **3** are shown in Scheme 1.

Complexes **1**, **2** and **3** in the crystalline form appear to be stable in air indefinitely. They are insoluble in alcohols (CH_3OH, C_2H_5OH, and *i*-PrOH), acetonitrile, and dimethyl sulfoxide (DMSO), but they dissolve readily in water.

3.2. X-ray crystallographic structures

The X-ray crystal structures of **1**, **2** and **3** consist of discrete anions and cations. Complexes **1** and **2** each crystallize in the triclinic system $P\bar{1}$ with two molecules per unit cell. Complex **3** crystallizes in the monoclinic space group $C2/c$ with eight molecules per unit cell. Selected interatomic distances and angles for **1**, **2** and **3** are given in Tables 2–4,

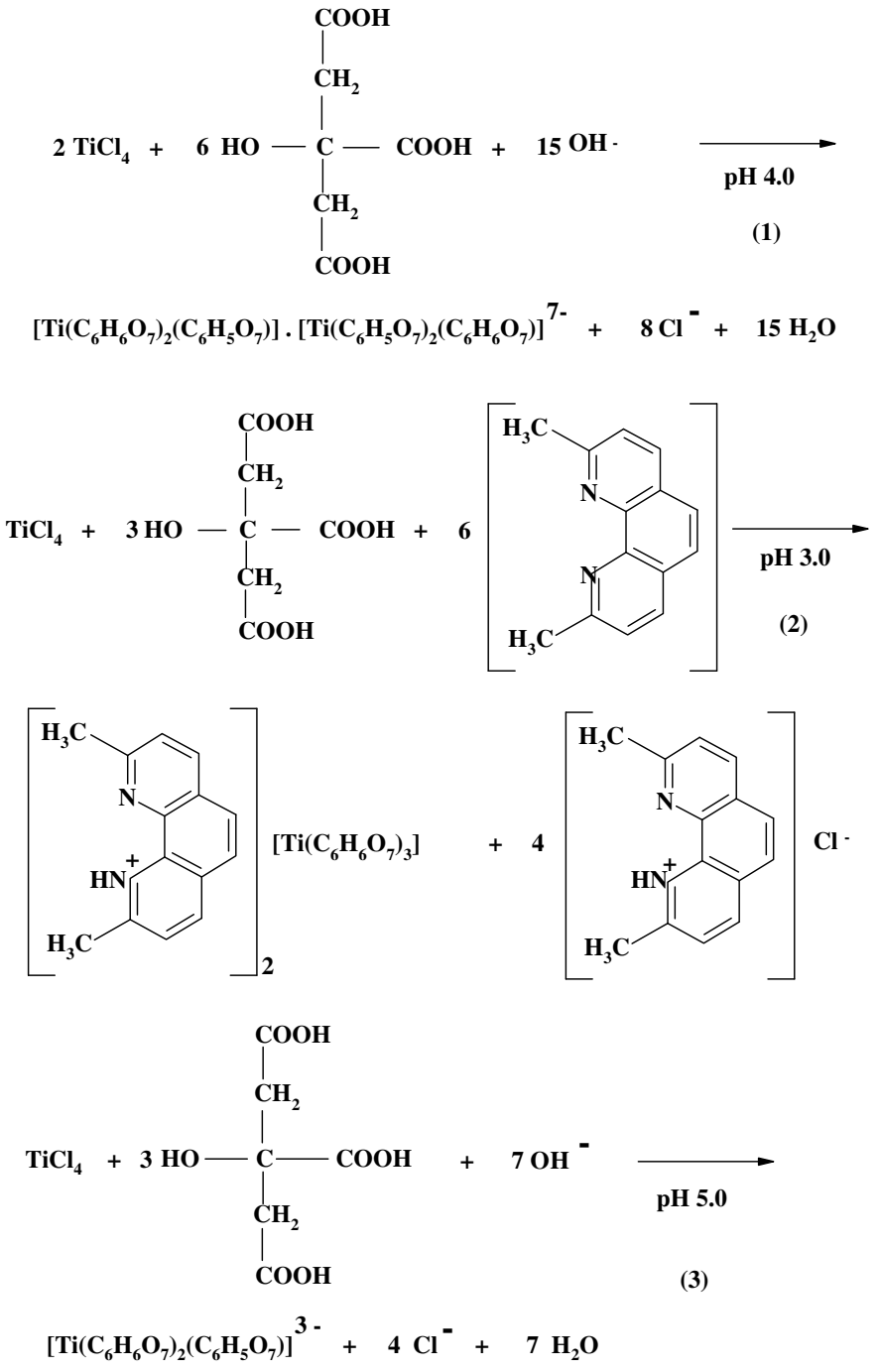

Scheme 1.

respectively. The ORTEP diagram of the anions in **1** is shown in Fig. 1. The anionic complexes **1A**, **1B**, **2** and **3** are mononuclear assemblies, each containing a Ti(IV) ion core with three coordinated citrate ligands. Each citrate ligand, in all anionic assemblies, binds to the central metal ion through the central alkoxide and carboxylate oxygens, generating a stable five-membered metallacyclic ring. The two terminal carboxylate groups of each citrate ligand in both **1A** and **1B**, **2** and **3** anions do not participate in coordination to the Ti(IV) ion. With three citrates bound to each Ti(IV) ion, the coordination number around that metal ion is six and the concomitant geometry is distorted octahedral in all anionic species. What is of great importance, however, in these mononuclear structural entities is the fact that not all of the bound citrates in each central metal ion possess the same deprotonation state. Specifically, in **1A** and **3**, two of the bound citrates are doubly deprotonated and the third one is triply deprotonated. As a result, the total charge of the complex is 3−. In **1B**, two of the bound citrates are triply deprotonated and the third one is doubly deprotonated. As a result, the total charge of the complex is 4−. In **2**, all three bound citrates

Table 2
Selected bond lengths [Å] and angles [°] in **1**

Molecule **1A**		Molecule **1B**	
Distances (Å)			
Ti(1)–O(23)	1.871(2)	Ti(2)–O(43)	1.860(2)
Ti(1)–O(13)	1.872(3)	Ti(2)–O(53)	1.865(2)
Ti(1)–O(3)	1.873(3)	Ti(2)–O(33)	1.868(2)
Ti(1)–O(5)	2.034(3)	Ti(2)–O(35)	2.041(3)
Ti(1)–O(15)	2.040(3)	Ti(2)–O(45)	2.048(3)
Ti(1)–O(25)	2.060(3)	Ti(2)–O(55)	2.048(3)
Angles (°)			
O(23)–Ti(1)–O(13)	92.9(1)	O(43)–Ti(2)–O(53)	95.1(1)
O(23)–Ti(1)–O(3)	92.2(1)	O(43)–Ti(2)–O(33)	95.4(1)
O(13)–Ti(1)–O(3)	93.0(1)	O(53)–Ti(2)–O(33)	93.3(1)
O(23)–Ti(1)–O(5)	156.0(1)	O(43)–Ti(2)–O(35)	104.5(1)
O(13)–Ti(1)–O(5)	109.6(1)	O(53)–Ti(2)–O(35)	159.5(1)
O(3)–Ti(1)–O(5)	78.7(1)	O(33)–Ti(2)–O(35)	78.9(1)
O(23)–Ti(1)–O(15)	109.6(1)	O(43)–Ti(2)–O(45)	79.3(1)
O(13)–Ti(1)–O(15)	79.1(1)	O(53)–Ti(2)–O(45)	106.5(1)
O(3)–Ti(1)–O(15)	157.0(1)	O(33)–Ti(2)–O(45)	159.8(1)
O(5)–Ti(1)–O(15)	83.7(1)	O(35)–Ti(2)–O(45)	83.5(1)
O(23)–Ti(1)–O(25)	78.9(1)	O(43)–Ti(2)–O(55)	158.5(1)
O(13)–Ti(1)–O(25)	156.2(1)	O(53)–Ti(2)–O(55)	79.1(1)
O(3)–Ti(1)–O(25)	109.5(1)	O(33)–Ti(2)–O(55)	105.5(1)
O(5)–Ti(1)–O(25)	83.3(1)	O(35)–Ti(2)–O(55)	84.7(1)
O(15)–Ti(1)–O(25)	82.7(1)	O(45)–Ti(2)–O(55)	82.5(1)

Table 3
Selected bond lengths [Å] and angles [°] in **2**

Distances (Å)			
Ti–O(13)	1.875(2)	Ti–O(15)	2.001(2)
Ti–O(3)	1.886(2)	Ti–O(5)	2.010(2)
Ti–O(23)	1.912(2)	Ti–O(25)	2.014(2)
Angles (°)			
O(13)–Ti–O(3)	93.6(1)	O(23)–Ti–O(5)	164.1(1)
O(13)–Ti–O(23)	90.4(1)	O(15)–Ti–O(5)	85.1(1)
O(3)–Ti–O(23)	95.0(1)	O(13)–Ti–O(25)	161.2(1)
O(13)–Ti–O(15)	79.8(1)	O(3)–Ti–O(25)	102.6(1)
O(3)–Ti–O(15)	160.6(1)	O(23)–Ti–O(25)	78.9(1)
O(23)–Ti–O(15)	103.1(1)	O(15)–Ti–O(25)	87.7(1)
O(13)–Ti–O(5)	104.6(1)	O(5)–Ti–O(25)	88.0(1)
O(3)–Ti–O(5)	79.0(1)		

Table 4
Selected bond lengths [Å] and angles [°] in **3**

Distances (Å)			
Ti–O(13)	1.861(2)	Ti–O(15)	2.064(2)
Ti–O(3)	1.873(2)	Ti–O(5)	2.046(2)
Ti–O(23)	1.866(2)	Ti–O(25)	2.063(2)
Angles (°)			
O(13)–Ti–O(3)	96.96(10)	O(23)–Ti–O(5)	100.06(11)
O(13)–Ti–O(23)	99.44(10)	O(15)–Ti–O(5)	83.17(10)
O(3)–Ti–O(23)	97.50(10)	O(13)–Ti–O(25)	100.39(10)
O(13)–Ti–O(15)	78.81(9)	O(3)–Ti–O(25)	162.63(10)
O(3)–Ti–O(15)	101.69(10)	O(23)–Ti–O(25)	78.83(10)
O(23)–Ti–O(15)	160.80(10)	O(15)–Ti–O(25)	82.68(9)
O(13)–Ti–O(5)	160.46(10)	O(5)–Ti–O(25)	84.64(10)
O(3)–Ti–O(5)	79.27(9)		

are doubly deprotonated. Regardless, however, of the degree of deprotonation of the citrate ligands in all Ti(IV) complexes, it is worth noting that the site of (de)protonation is the terminal carboxylate group(s) of the citrates not participating in coordination around the central metal ion.

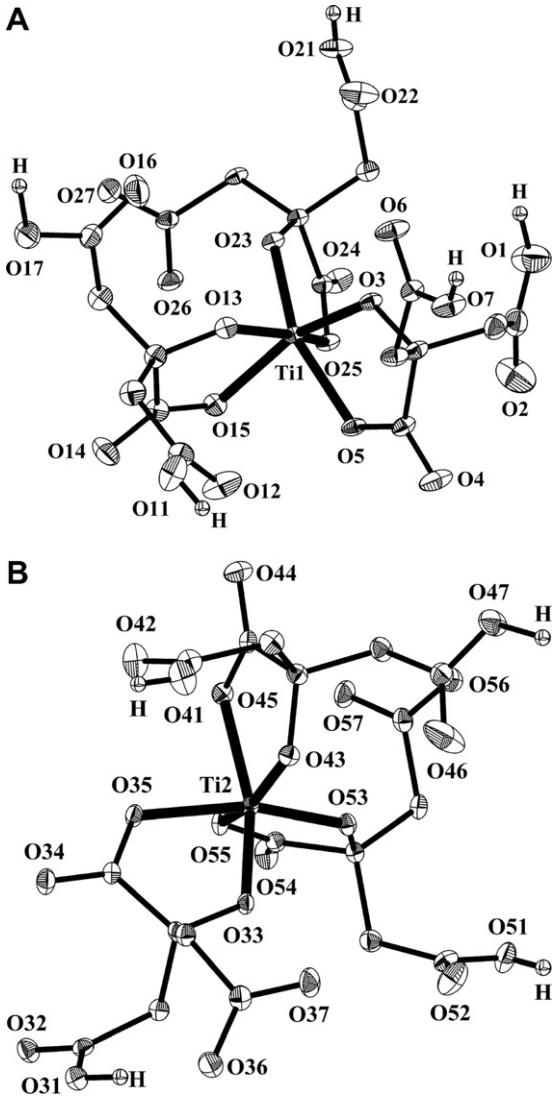

Fig. 1. Partially labelled ORTEP plot of the $[Ti(C_6H_6O_7)_2(C_6H_5O_7)]^{3-}$ (**1A**) and $[Ti(C_6H_5O_7)_2(C_6H_6O_7)]^{4-}$ (**1B**) anions with the atom labelling scheme in **1**. Thermal ellipsoids are drawn by ORTEP and represent 30% probability surfaces.

The Ti–O bond distances in **1**, **2** and **3** are in line with those in other Ti(IV)–O_6 oxygen-containing complexes, such as $Na_6[Ti(C_6H_{4.5}O_7)_2(C_6H_5O_7)] \cdot 16H_2O$ (**4**) (1.852(3)–2.055(3) Å) and $Na_3(NH_4)_3[Ti(C_6H_{4.5}O_7)_2(C_6H_5O_7)] \cdot 9H_2O$ (**5**) (1.860(3)–2.061(4) Å) [24], $Na_8[Ti(C_6H_4O_7)_3] \cdot 17H_2O$ (**6**) (1.833(2)–2.076(2) Å) [25], $Na_4[Ti_2O_5(C_6H_6O_6N)_2] \cdot 11H_2O$ (**7**) (1.819(2)–2.065(2) Å) [26], $(NH_4)_2[TiO(C_2O_4)_2] \cdot H_2O$ (**8**) (1.785(7)–1.855(6) Å) [27], $Cs_4[Ti_4O_4(C_6H_6NO_6)_4] \cdot 6H_2O$ (**9**) (1.74(1)–2.02(1) Å) [28], $K_2[Ti_2O_5(C_7H_3O_4N)_2] \cdot 5H_2O$ (**10**) (1.825(2)–2.183(7) Å) [29], $(NH_4)_8[Ti_4(C_6H_4O_7)_4(O_2)_4] \cdot 8H_2O$ (**11**) (1.863(1)–2.085(1) Å) [21], $(NH_4)_4[Ti_2(O_2)_2(C_6H_4O_7)_4] \cdot 2H_2O$ (**12**) (1.852(2)–2.085(2) Å) [20], and $KMg_{1/2}[Ti(H_2cit)_3] \cdot 6H_2O$ (**13**) (1.865(1)–2.045(1) Å) [19]. Species **13**

has been reported to contain doubly deprotonated citrates bound to the Ti(IV) metal ion. It appears that similar angles are observed in **1** and a number of $Ti^{IV}O_6$ core-containing complexes, exhibiting octahedral geometry around the Ti(IV) ions. Among such complexes are **(8)** (77.1(3)–171.2(12)°) and $KMg_{1/2}[Ti(H_2cit)_3]\cdot 6H_2O$ (**13**) (79.99(4)–156.52(5)°) [19].

In a series of anionic mononuclear metal–citrate complexes reported in the past [30–34], the triply and fully deprotonated citrate ligands adopt an extended conformation upon binding to the metal ion. As a result, the carbon atoms C(1), C(2), C(3), C(5), and C(6) of the citrate backbone are coplanar. It appears, however, that this structural attribute does not apply in the case of the Ti(IV)–citrate congener species. Specifically, the citrate ligands in the anions of **1A** and **1B** adopt a 'bend' conformation (i.e. the carbon atoms C(1), C(2), C(3), C(5), and C(6) of the citrate backbone are not coplanar) upon binding to the titanium ion. In both, the doubly and triply deprotonated citrates, the carbon of the terminal protonated carboxylate is displaced by ~1.1 Å out of the best mean plane of the remaining four carbon atoms defining the citrate backbone. This fact may be attributed to the participation of the corresponding carboxylate in strong inter-molecular hydrogen-bonding interactions (O(7)···O(36) = 2.579 Å, O(17)···O(27) = 2.586 Å, O(21)···O(6) = 2.640 Å, O(47)···O(56) = 2.549 Å, O(51)···O(37) = 2.630 Å) (Table 5). In the case of the triply deprotonated citrate containing C(31), C(32), C(33), C(35), and C(36), the 'bending' is even larger (C(31) is displaced by ~1.6 Å out of the best mean plane of the remaining four carbons), a fact attributed to the strong intra-molecular hydrogen bond between the terminal carboxylates (O(31)···O(36) = 2.656 Å) (Table 5). The central carboxylate plane in **1A**, O(4)–C(4)–O(5), is rotated ~3.8° out of the O(3)–C(3)–C(4) plane. The corresponding values for the remainding two Ti(IV)-bound citrates are ~13.0° and ~11.5°, respectively. In **1B**, the central carboxylate plane O(34)–C(34)–O(35) is rotated ~2.5° out of the O(33)–C(33)–C(34) plane. An analogous geometric account (~9.3° and ~9.5°, respectively) is also valid for the additional two citrates bound around Ti(IV).

The aforementioned observations hold equally well in the case of the anion in **2**. There, carbon atom C(6) is displaced out of the best mean plane of the remaining four carbon atoms C(1), C(2), C(3), C(5) by 1.55 Å. The corresponding displacement of the carbon atoms C(16) and C(26) in the other two citrate ligands in **2** is 1.52 Å and 1.25 Å, respectively. Here as well, a plausible explanation for this phenomenon may be the participation of the corresponding carboxylate oxygens in strong intra-molecular (O(7)···O(3) = 2.552 Å, O(17)···O(23) = 2.688 Å) and inter-molecular (O(27)···OW(5) = 2.658 Å) hydrogen-bonding interactions, which force the carboxylate moieties to bend with respect to the citrate backbone (Table 6). The central carboxylate plane O(4)–C(4)–O(5) for the first citrate is rotated ~6.6° out of the O(3)–C(3)–C(4) plane, the central carboxylate plane O(14)–C(14)–O(15) for the second citrate is rotated ~14.0° out of the O(13)–C(13)–C(14) plane, and the central carboxylate plane O(24)–C(24)–O(25) for the third citrate is rotated ~7.4° out of the O(23)–C(23)–C(24) plane.

Analogous observations were made in the case of the anion in **3**. There, carbon atom C(1) is displaced out of the best mean plane of the remaining four carbon atoms C(2), C(3), C(5), C(6) by 1.14 Å. The corresponding displacement of the carbon atoms C(11) and C(26) in the other two citrate ligands in **3** is 1.27 Å and 1.11 Å, respectively. Here as well, a plausible explanation for this phenomenon may be the participation of the corresponding carboxylate oxygens in strong inter-molecular (O(7)···OW(1) = 2.712 Å, O(11)···O(2) = 2.604 Å, O(27)···O(1) = 2.573 Å) hydrogen-bonding interactions, which force the carboxylate moieties to bend with respect to the citrate backbone (Table 7). The central carboxylate plane O(4)–C(4)–O(5) for the first citrate is rotated ~5.2° out of the O(3)–C(3)–C(4) plane, the central carboxylate plane

Table 5
Hydrogen-bonding interactions in complex **1**

Interaction	D···A (Å)	H···A (Å)	D–H···A (°)	Symmetry code
O1–HO1···W7′	3.510	2.359	177.0	$-x, 2-y, 1-z$
O7–HO7···O36	2.579	1.915	177.0	$1-x, 1-y, 2-z$
O11–HO11···W4′	2.689	1.866	163.4	$-x, 1-y, 1-z$
O17–HO17···O27′	2.586	1.475	172.1	$-1-x, 2-y, 1-z$
O21–HO21···O6′	2.640	1.929	171.0	$-x, 2-y, 1-z$
O31–HO31···O36	2.656	1.794	174.1	x, y, z
O41–HO41···W2′	2.617	1.829	173.8	$x, -1+y, 1+z$
O47–HO47···O56′	2.549	1.399	165.9	$-x, 1-y, 2-z$
O51–HO51···O37′	2.630	1.881	169.4	$1-x, 1-y, 2-x$
W1–HW1A···O55′	2.900	2.233	158.0	$1-x, 1-y, 1-z$
W1–HI1B···O35′	2.837	2.063	164.9	$x, 1+y, -1+z$
W2–HW2A···O27′	2.688	1.865	173.1	$1+x, y, z$
W2–HW2B···W7′	2.930	2.430	154.0	$-x, 2-y, 1-z$
W4–HW4A···W6′	2.929	2.331	170.2	$x, y, -1+z$
W4–HW4B···O56′	2.659	1.699	169.5	$-x, 1-y, 1-z$
W9–HW9A···O14′	2.785	1.887	164.8	$-x, 1-y, 1-z$

Table 6
Hydrogen-bonding interactions in complex **2**

Interaction	D···A (Å)	H···A (Å)	D–H···A (°)	Symmetry code
O1–HO1···O2′	2.634	1.747	171.3	$1-x, 1-y, 2-z$
O21–HO21···OW1′	2.723	1.812	167.8	$x, 1+y, 1+z$
O11–HO11···O4′	2.592	1.676	158.8	$-x, 1-y, 2-z$
O17–HO17···O23	2.688	1.660	170.1	x, y, z
N2–HN2···O6	2.797	2.019	159.7	x, y, z

O(14)–C(14)–O(15) for the second citrate is rotated ~5.0° out of the O(13)–C(13)–C(14) plane, and the central carboxylate plane O(24)–C(24)–O(25) for the third citrate is rotated ~2.1° out of the O(23)–C(23)–C(24) plane.

Three potassium counter ions in **1A** and four potassium counter ions in **1B** are also present in the lattice of **1**. They counterbalance the total 7− charge generated. The potassium cations are in contact with the carboxylate oxygens of the citrate anion as well as the lattice water oxygens at distances in the range 2.645(3)–3.084(3) Å. The presence of the terminal protonated carboxylates in the structure of **1** along with the lattice water molecules plays an important role in the development of the lattice structure of the compound. The anions of **1A** are hydrogen-bonded through O(17)–HO(17)···O(27) and O(21)–HO(21)···O(6) to form zig-zag chains running along the crystallographic *a*-axis (Fig. 2A). In an analogous manner, the anions of **1B** are connected through hydrogen-bonding interactions (O(47)–HO(47)···O(56) and O(51)–HO(51)···O(37)) leading to zig-zag chains developed along the crystallographic *a*-axis (Fig. 2B). These two zig-zag chains are linked through the O(7)–HO(7)···O(36) hydrogen bond, and form layers parallel to the *ac* plane. The remaining protonated citrate carboxylates are involved in H-bonds, with the water molecules of crystallization (Table 5) assisting the establishment of an extensive hydrogen-bonding network.

The presence of the protonated terminal carboxylates and their participation in hydrogen-bonding interactions also play an important role in the overall structure of **2** (Table 6). In particular, two adjacent mononuclear anions are doubly hydrogen-bonded through O(11)–HO(11)···O(4′) forming dinuclear units. In turn, the latter units are further doubly hydrogen-bonded through O(1)–HO(1)···O(2′), forming polymeric chains extended along the crystallographic *b* axis (Fig. 3). Two 2,9-dimethyl-1,10-phenanthrolinium counter ions and five water molecules of crystallization per mononuclear anion are present in the lattice of **2**. The counter ions are singly charged and their chemical identity supports (a) their role as derivatives of the original neocuproine base, and (b) their participation as bulky counter ions stabilizing the lattice of **2** through hydrogen-bonding interactions involving the water molecules of crystallization (N(3)···OW(3) = 2.795 Å) and terminal carboxylate oxygens (N(2)···O(6) = 2.797 Å). The cations and the lattice water molecules as well as the carboxylate oxygens of the citrate ligands are in contact (interatomic distances in the range 2.659–3.220 Å), establishing an extensive hydrogen-bonding network, responsible for the stability of the crystal lattice in **2**.

There are four crystallographically independent sodium ions in the structure of **3**, two of which (Na(1) and Na(2)) are sitting on general positions and presenting distorted octahedral coordination geometry comprising water molecules of crystallization and carboxylate oxygen anchors in the range of 2.325–2.455 Å. The third sodium ion (Na(3)) is disordered around a twofold axis of symmetry, and it is coordinated to four water molecules of crystallization and carboxylate oxygen anchors in the range 2.232–2.324 Å. The fourth sodium ion (Na(4)) is disordered around a center of symmetry and coordinated to five water

Table 7
Hydrogen-bonding interactions in complex **3**

Interaction	D···A (Å)	H···A (Å)	D–H···A (°)	Symmetry code
O7–HO7···OW1′	2.712	1.929	164.1	$0.5-x, 0.5-y, 1-z$
O11–HO11···O2′	2.604	1.814	171.7	$1-x, -y, 1-z$
O17–HO17···Ow3′	2.675	1.432	162.3	$1-x, -y, 1-z$
O21–HO21···OW2′	2.686	1.781	173.3	$1-x, 1-y, 1-z$
O27–HO27···O1′	2.573	1.452	167.5	$1.5-x, 0.5-y, 1-z$
OW1–HW1A···O14′	2.832	2.095	164.2	$0.5-x, 0.5-y, 1-z$
OW1–HW1B···O15′	2.820	1.991	163.0	$-0.5+x, 0.5-y, -0.5+z$
OW2–HW2A···O25′	2.800	2.076	167.4	$-0.5+x, 0.5-y, -0.5+z$
OW2–HW2B···O4′	2.835	2.115	165.4	$1-x, 1-y, 1-z$
OW3–HW3A···O5′	2.798	2.040	178.9	$-0.5+x, 0.5-y, -0.5+z$
OW3–HW3B···O24′	2.788	1.914	169.1	$1-x, -y, 1-z$
OW4–HW4A···OW10′	2.333	1.507	161.0	$-1+x, y, -1+z$
OW6–H6A···O4′	2.922	1.890	146.5	$0.5-x, 1.5-y, 1-z$
OW6–HW6B···O24′	2.902	1.853	158.7	$1-x, 1-y, 1-z$

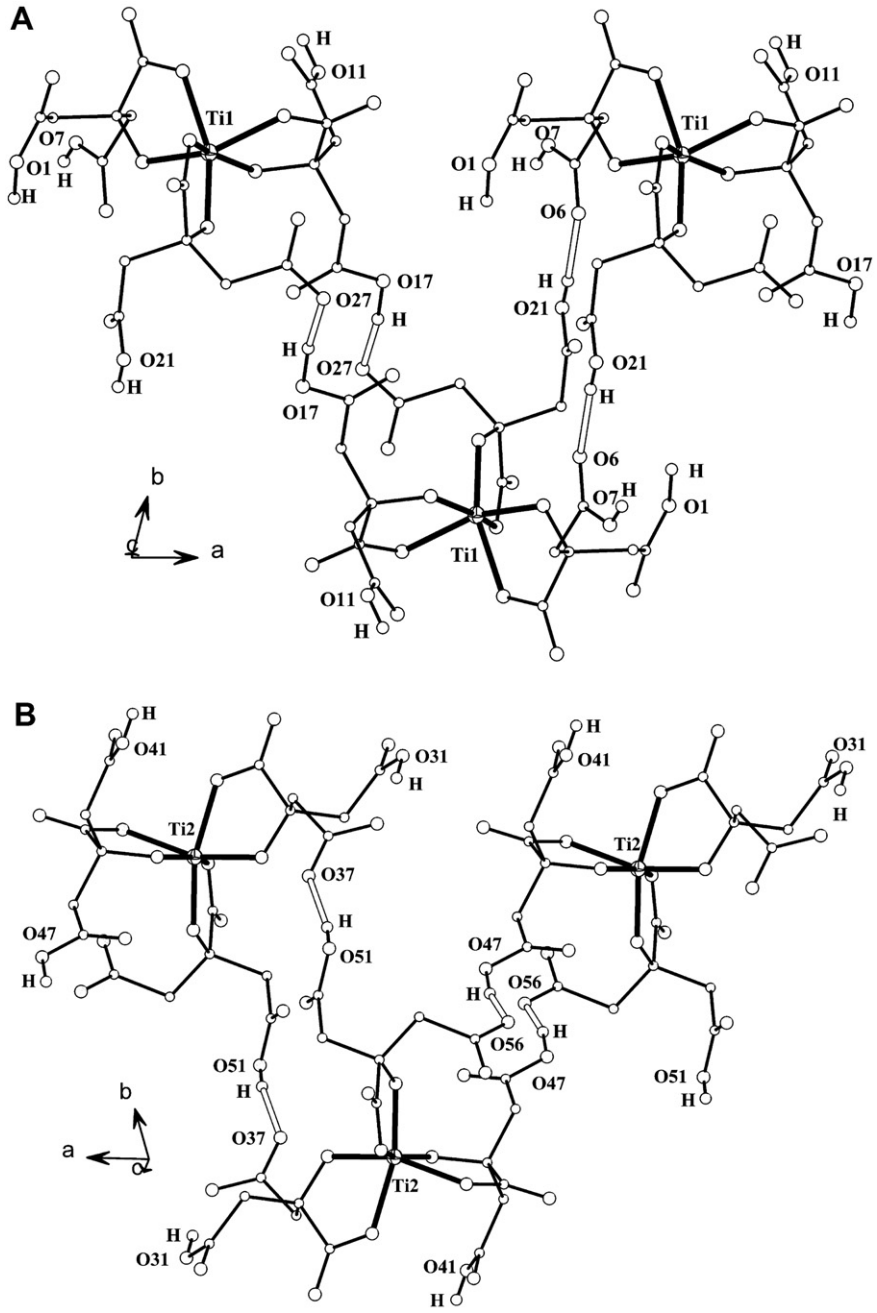

Fig. 2. Partially labelled ORTEP diagram showing the formation of the zig-zag chains of **1A** (A) and **1B** (B) along the *a*-axis, through hydrogen-bonding interactions (open bonds). Hydrogen atoms (smaller circles) for the carbon citrates have been omitted for clarity.

molecules of crystallization and carboxylate oxygen anchors in the range 2.154–2.518 Å. Hydrogen-bonding interactions through O(11)–HO(11)···O(2) as well as Na–O coordination bonds in the lattice structure of **3** are responsible for the formation of heterometallic tetranuclear Ti_2Na_2 units, which are further hydrogen-bonded through O(27)–HO(27)···O(1) to form chains (Fig. 4). The overall lattice structure of **3** is further stabilized by the Na–O coordination bonds and the hydrogen-bonding interactions between the water molecules of crystallization and carboxylate oxygen anchors.

3.3. FT-IR spectroscopy

The FT-Infrared spectra of **1**, **2** and **3** in KBr revealed the presence of vibrationally active carboxylate groups. Antisymmetric as well as symmetric vibrations for the carboxylate groups of the coordinated citrate ligands dominated the spectrum. Specifically, antisymmetric stretching vibrations $\nu_{as}(COO^-)$ were present for the carboxylate carbonyls in the range 1709–1639 cm^{-1} for **1**, 1731–1707 cm^{-1} for **2**, and 1702–1626 cm^{-1} for **3**, respectively. Symmetric vibrations $\nu_s(COO^-)$ for the same groups were present in

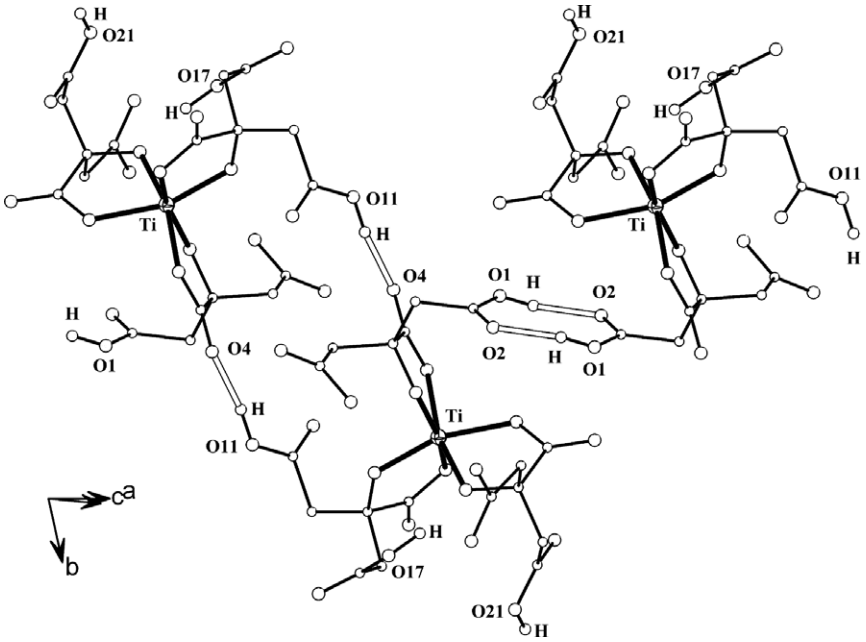

Fig. 3. Partially labelled ORTEP plot of **2**, showing the hydrogen-bonding network of chains of dimers assembled along the *b* axis. Only H-atoms participating in H-bond formation are shown. The organic counter ions are omitted for clarity.

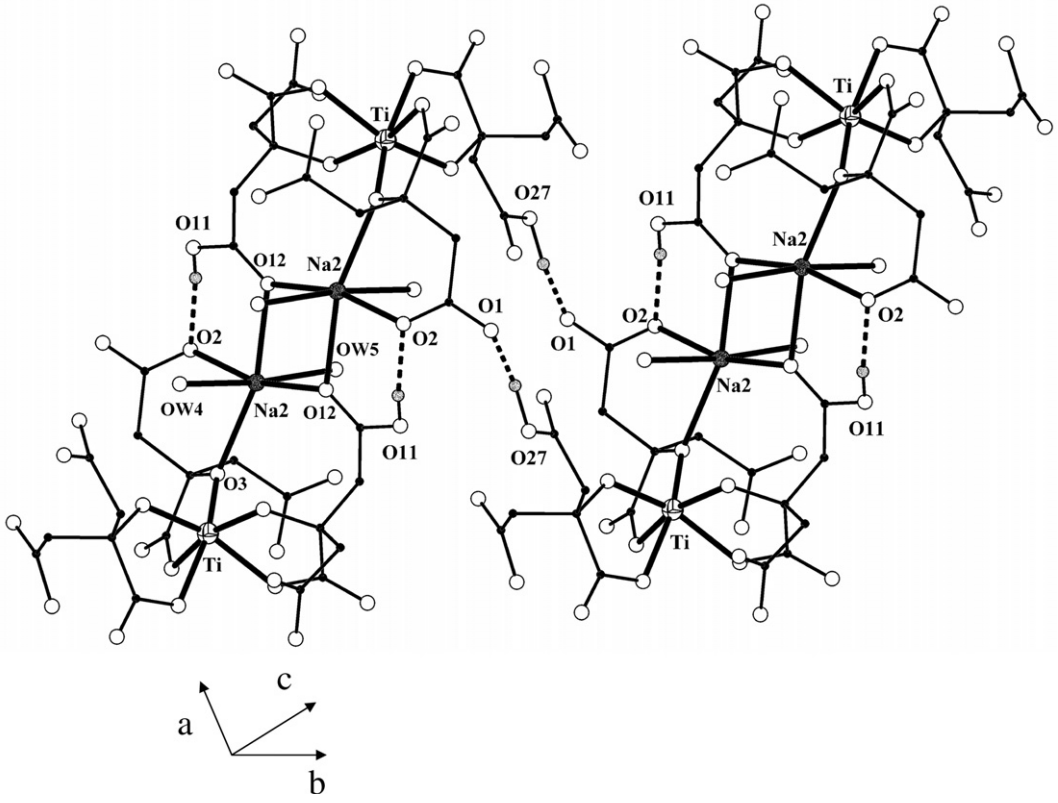

Fig. 4. Partially labelled ORTEP plot of **3** showing only the hydrogen-bonding network described in the text.

the range 1435–1306 cm^{-1} for **1**, 1626–1604 cm^{-1} for **2**, and 1414–1300 cm^{-1} for **3**, respectively. The frequencies of the observed carbonyl vibrations were shifted to lower values in comparison to the corresponding vibrations in free citric acid, indicating changes in the vibrational status of the citrate ligand upon coordination to titanium [35]. These changes were reflected in the coordination of the citrate ligand to the metal ion. Confirmation of this contention

came from the X-ray crystal structures of **1**, **2**, and **3**. All of the aforementioned assignments were in agreement with previous assignments in mononuclear Ti(IV)–O_6 [36] complexes, and in line with prior reports on carboxylate containing ligands bound to different metal ions [37,38].

3.4. Solid-state NMR spectroscopy

The solid-state MAS ^{13}C NMR spectrum of **3** (Fig. 5A top) was in line with the coordination mode of citrate around the Ti(IV) ion. The spectrum showed four separate peak features. In the high field region there appear to be two resonances, whereas the other two emerge in the low field region. The resonances in the high field region could be attributed to the two methylene carbons (42.8–45.8 ppm) located next to the coordinated carboxylates of the citrate ligand. The resonance in 90.1–91.7 ppm is reasonably assigned to the central carbon atom located adjacent to the bound central carboxylate group. In the low field region, where the carbonyl carbon resonances are expected, the observed (173.6–178.0 ppm) features correspond to the terminal carboxylate groups. The observed resonances at even lower fields (188.7–189.8 ppm) could be assigned to the bound central carboxylate carbon of the citrate ligand. This signal is shifted downfield by more than 12 ppm in comparison to the previous signal for the terminal carboxylate groups, most likely due to the presence of the nearby ionized alkoxide group. A similar pattern of ^{13}C resonances was observed in the case of mononuclear complexes, such as $Na_6[Ti(C_6H_{4.5}O_7)_2(C_6H_5O_7)] \cdot 16H_2O$ (**4**) [24], $(NH_4)_5[Al(C_6H_4O_7)_2] \cdot 2H_2O$ [34], the tetranuclear complex $(NH_4)_8[Ti_4(C_6H_4O_7)_4(O_2)_4] \cdot 8H_2O$ (**11**) [21], and dinuclear complexes such as $Na_2[Bi_2(C_6H_4O_7)_2] \cdot 7H_2O$ [39].

3.5. Solution NMR spectroscopy

The solution ^{13}C NMR spectrum of complex **3** was recorded in D_2O (Fig. 5A bottom). The spectrum showed several sets of resonances. The resonances in the high field region (44.3–46.1 ppm) were attributed to the CH_2 groups of the citrate ligands bound to the central Ti(IV) ion. The resonance at 91.1 ppm was assigned to the central carbon of the bound citrate. The signals in the lower field region 177.2–177.4 ppm were assigned to the terminal carboxylate carbons coordinated to the Ti(IV) central ion. The resonance located at the low end of the field (188.5 ppm) was attributed to the central carboxylate carbon attached to the Ti(IV) ion. This signal was shifted to lower fields in comparison to the other signal belonging to the terminal carboxylate carbons. The shift was ~11.0 ppm downfield and was comparable to the one observed in the MAS ^{13}C solid-state spectrum of **3**. Here as well, the shift was most likely due to the presence of the central carboxylate carbon close to the deprotonated alkoxide group of the Ti(IV) coordinated citrates. It is worth emphasizing that this

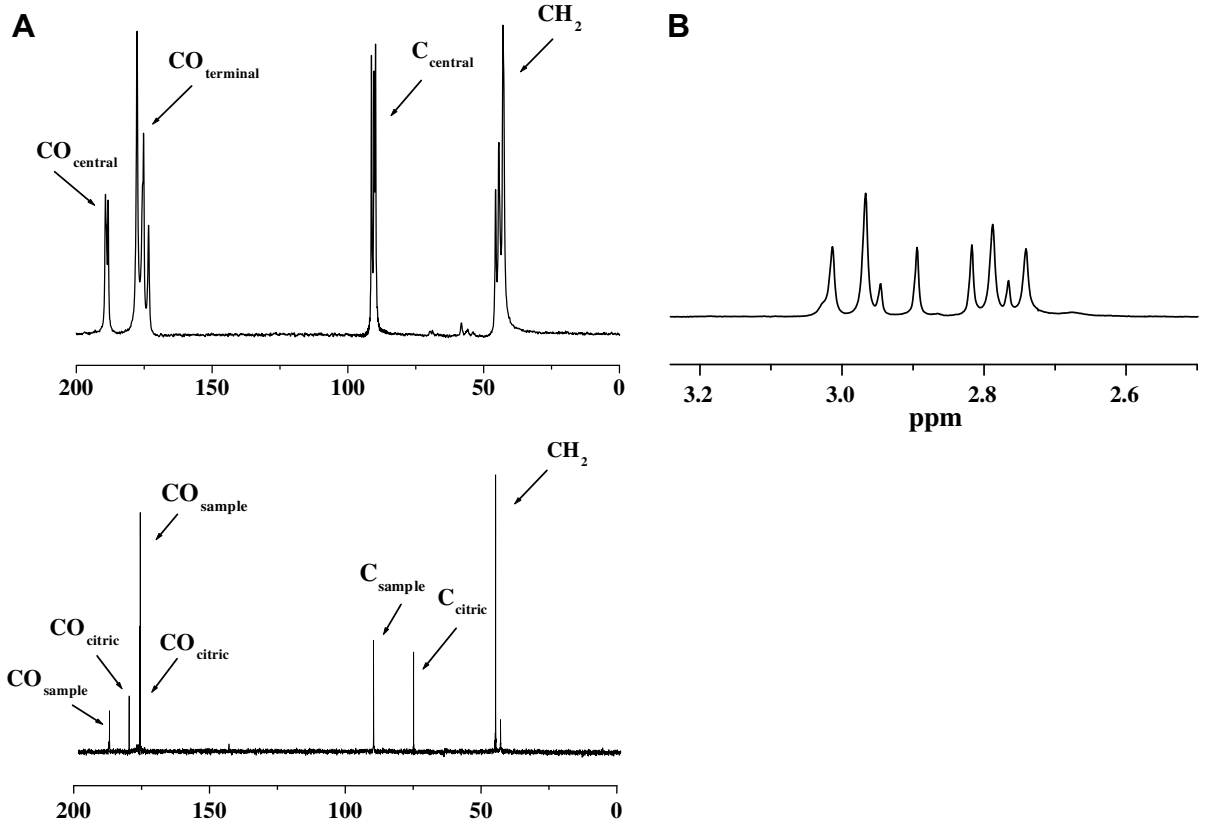

Fig. 5. (A) ^{13}C MAS NMR solid-state (top) and ^{13}C NMR solution (bottom) spectrum of **3**. (B) ^{1}H NMR spectrum of **3** in D_2O solution.

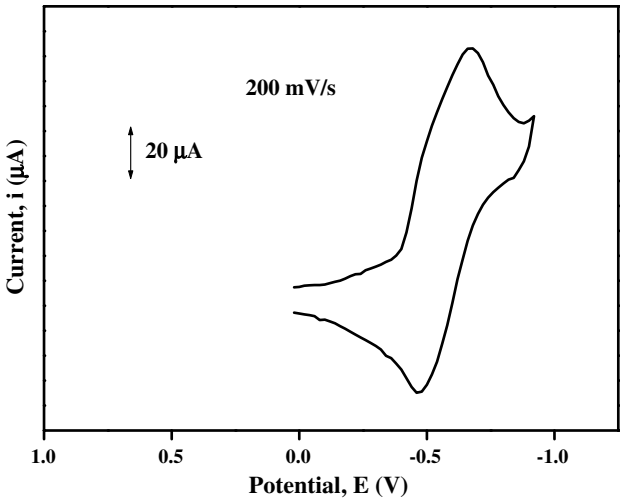

Fig. 6. Cyclic voltammetric trace of complex **2** in aqueous solution.

pattern of resonances observed in solution for **3**, was similar to that observed in the solid-state ^{13}C MAS NMR spectrum of the same species. It appears, therefore, that there is a consistency between the solid and solution state spectra. Furthermore, the additional set of observed resonances in the same spectrum was easily attributed to the presence of free citrate, suggesting the dissociation of the complex in solution. In support of this picture, the ^{1}H NMR spectrum of complex **3** (Fig. 5B) shows two groups of sharp AB quartets for the methylene protons. This solution behavior has been observed before [24] with the exhibited patterns supporting the idea of dissociation of the Ti(IV)–citrate complex in aqueous solution, releasing free citrate.

3.6. Cyclic voltammetry

Electrochemical measurements were taken for **2** in water, in the presence of KNO_3 as a supporting electrolyte. The cyclic voltammogram showed a one-electron redox wave at $E_{1/2} = -0.57$ V ($\Delta E = 180$ mV, $ip_a/ip_c = 1.0$, $ip_c/\{(v)^{1/2}C\}$ constant) that corresponds to the Ti(III)/Ti(IV) redox couple (Fig. 6). The observed $E_{1/2}$ value is comparable to, yet lower than, the one reported for Ti(III)–citrate preparations at pH 7. Attempts to pursue the isolation of the one-electron reduced product of the title complex **2** are currently ongoing.

4. Discussion

4.1. The multicomponent binary Ti(IV)–citrate aqueous system

The employment of pH-dependent chemistry in the synthesis of three Ti(IV)–citrate mononuclear species in the binary Ti(IV)–citrate system was instrumental in the successful pursuit of the present work. Complexes **1**, **2**, and **3** were synthesized in the pH range from 3 to 5 in water. In compound **1**, an unusual case of co-crystallization of two species was achieved at pH 4, while in the other two compounds the anionic complex was isolated in the presence of different cations albeit at slightly different pH values. Specifically, in **1**, the anionic species $[Ti(C_6H_6O_7)_2(C_6H_5O_7)]^{3-}$ (**1A**) and $[Ti(C_6H_5O_7)_2(C_6H_6O_7)]^{4-}$ (**1B**) emerged as the dominant components, whereas in the case of compounds **2** and **3** discrete $[Ti(C_6H_nO_7)_2(C_6H_q\ O_7)]^{p-}$ ($n = 6$, $q = 6$, $p = 2$ (**2**); $n = 6$, $q = 5$, $p = 3$ (**3**)) were present in each case. In the latter species, the counter ions Na^+ and $(C_{14}H_{13}N_2)^+$ were critical in achieving their isolation. Thus, in all cases, cations were essential in the isolation of the arisen species upon precipitation with alcohol or slow evaporation. Concurrently, as a result of the variable (de)protonation state of the citrates around Ti(IV), the charge of the arising species **1**, **2** and **3** varied in an analogous fashion. To this end, it appears that (a) the basic core of the arising complexes in the Ti(IV)–citrate system under the presently employed conditions is retained throughout the investigated pH range, and (b) pH-dependent chemistry occurs in the periphery of the core and develops specifically as a (de)protonation process on the terminal carboxylates of the Ti(IV)-bound citrates. The employed physicochemical techniques (X-rays, FT-IR, MAS NMR and solution NMR) attest to the above properties and support a clear picture of the solid-state and solution properties of all species examined.

In light of the aforementioned, it appears that the number of discrete species arisen through pH-dependent chemistry of the Ti(IV)–citrate system carried out so far project certain systematic observations. Specifically, in all of the cases-species examined thus far: (a) there was one point clear about the nature of the complexes isolated from solution and characterized; they were all discrete mononuclear complexes, (b) all the species were octahedral in nature, containing Ti(IV) with three citrate ligands attached to them, (c) the citrates bound Ti(IV) through the central carboxylate and alkoxide moieties, stabilizing the arising complex through formation of a stable five-member metallacyclic ring, (d) the diverse nature of the arisen species was exemplified through the variable (de)protonation state of the terminal carboxylate groups of the Ti(IV)-bound citrate ligands, and (e) there was a strong influence of the employed base (and hence counter ion) on the solubility of the arisen pH-structural variants species that could be isolated from solution. This profile certainly encompasses the properties of all species seen so far and isolated as discrete entities in their respective lattice. Herein, however, the aqueous synthetic chemistry of the Ti(IV)–citrate system has provided, in an expedient fashion, an "assembly" of species containing two pH Ti(IV)–citrate structural variants. The isolated crystalline product was composed of two distinct dinuclear complexes-subunits (**1A** and **1B**) (Fig. 1). That solid-state assembly, however, may not necessarily reflect the state of complex **1** in solution (*vide infra*). From the three-dimensional structure it is evident that the two component complexes of this large assembly could be discrete species themselves, existing in aqueous

solutions of the perused binary system. As discrete moieties, these species have now been isolated in the solid-state, including the anion in compound **3** [40]. Very likely, the complexity of this system is also reflected in other pH regions of this speciation scheme, one that challenges further synthetic investigations.

An important comparative correlation between Ti(IV)–citrates and other M(II/III)–citrates arises from the composition of the complexes themselves. Specifically, in complexes **1**, **2** and **3**, each citrate binding Ti(IV) occupies two sites in the metal coordination sphere. Hence, three citrates occupy all sites in the octahedral geometry formulated around Ti(IV). In contrast to this behavior, metal ions with oxidation states +2 and +3, M(III,II) ($[Al(C_6H_4O_7)_2]^{5-}$ [30], $[Al(C_6H_4O_7)(C_6H_5O_7)]^{4-}$ [34], $[Fe(C_6H_4O_7)_2]^{5-}$ [31], $[Mn(C_6H_4O_7)_2]^{5-}$ [33], and $[Mn(C_6H_5O_7)_2]^{4-}$ [33]), prefer two citrates in their coordination sphere. In it, each of the two citrates binds through the central carboxylate and alkoxide groups along with one of the terminal carboxylate groups. Collectively, then, it appears that the reduction of the oxidation state of the metal in the binary M(IV)–citrate system seems to lower the ligand to metal ratio while retaining the same coordination number and geometry. Further in-depth studies, however, are needed to validate this contention.

4.2. Links to Ti(IV)–citrate speciation

Compounds **1**–**3** reflect species in the binary Ti(IV)–citrate system and emphasize their importance as components of the system covering a specific pH range. Along with the other hitherto known species of $[Ti(C_6H_{4.5}O_7)_2(C_6H_5O_7)]^{6-}$ [24] and $[Ti(C_6H_4O_7)_3]^{8-}$ [25], they formulate a family of mononuclear species contributing to the speciation of the requisite system in the aqueous media. Knowing that the aqueous speciation involves a web of pH-dependent equilibria in the Ti(IV)–citrate system, the complexes isolated and characterized so far project (a) the nature of complexes participating in such a distribution, and (b) their structural diversity exemplified through the (de)protonation processes, selectively occurring at the non-participating carboxylate terminals of the bound citrates around Ti(IV). In this respect, apart from the discrete species **2** and **3**, compound **1** presents a rather unusual "picture" of a pH-specific slice of the aqueous distribution of the binary Ti(IV)–citrate system over the physiological pH range. That notion has been confirmed by the crystal structure of **3** and the recent isolation of the individual components in **1** [40]. To this end, considerable knowledge is gained that helps comprehend the composition of the speciation scheme of the requisite system.

The aforementioned species as pH-structural variants of a fundamental core assembly of Ti(IV)–O_6 reflect quite clearly the fact that the variability is associated with single proton abstraction processes occurring on the terminal carboxylate groups of the bound citrates. Bearing in mind that each bound citrate has two uncoordinated terminal groups capable of being deprotonated, the number of potential Ti(IV)–citrate variants is fairly large with the participant species in the distribution bearing charges from 2− to 8−; overall a six proton abstraction process. The aforementioned thesis is consistent with our previously proposed distribution of Ti(IV)–citrate species partaking of the aqueous speciation scheme of single-proton step processes in a pH-dependent fashion [24]. In light of the presently known species in the aqueous Ti(IV)–citrate speciation, the existence of other single (or potentially even double) proton pH-structural variants or higher nuclearity complexes cannot be ruled out.

Furthermore, the tris–chelate complexes of the Ti(IV)–O_6 core earmark the chemistry of interactions of that highly charged first transition series metal ion with physiologically important biomolecular targets. The fact that all the species in the requisite speciation scheme are soluble is a crucial piece of evidence potentially linking them with bioavailable Ti(IV) species participating/influencing (bio)chemical pathways in cellular processes. It is worth noting that such interactions are congruent with the previously suggested potential roles for titanium (e.g. composites in prosthetics) covering protein expression [41], growth factor recruitment [42], signal transduction [43], enzyme activation [44], gene expression [45,46], and others [47]. To this end, searching for elusive new and novel Ti(IV)–O_6 species linking their chemical identity with potential biological roles is currently ongoing in our labs.

4.3. Electrochemical considerations

Having the discrete binary Ti(IV)–citrate species $(C_{14}H_{13}N_2)_2[Ti(C_6H_6O_7)_3]\cdot 5H_2O$ (**2**) (pH 3) and $Na_3(NH_4)_3[Ti(C_6H_{4.5}O_7)_2(C_6H_5O_7)]\cdot 9H_2O$ (**5**) (pH 6) [24] available at different pH values was essential in (a) assessing their redox behavior in aqueous media at the autogenous pH, and (b) linking their redox behavior with the aqueous speciation scheme of the requisite binary Ti(IV)–citrate system. In this respect, the cyclic voltammetry of species **2** was studied in aqueous solution, and was subsequently compared with that of complex **5** [24] at the same concentration. This comparison led to specific trends in the redox behavior of pH-dependent binary structural Ti(IV)–citrate variants and their association with the known aqueous speciation of the respective system (Table 8). In the observed voltammograms for the two pH-structural variants, it appears that (a) as the pH of the aqueous solution increases, there is a decrease in the approximate half-wave potential of the binary Ti(IV)–citrate species. It is very likely that in the context of the aqueous speciation of the system, a rise in the pH increases the degree of deprotonation of bound citrate ligands, thus rendering the requisite species more negative and reducing the half-wave potential values for the Ti(IV)/Ti(III) redox couple versus NHE, (b) as the pH decreases there is a gain in chemical reversibility of species **2** versus species **5** (quasi-reversible) at a specific sweep rate, (c) at a specific pH

Table 8
Comparative cyclic voltammetric data for discrete Ti(IV)–citrate compounds at specific pH values

Compound	pH	E_{red} (mV)[a]	E_{ox} (mV)	$E_{1/2}$ (mV)	ΔE (mV)
2	3	−430 (−394)[b]	−226 (−230)	−328 (−312)	180 (164)
5	6	−401 (−427)	−308 (−354)	−355 (−391)	93 (73)

[a] E values listed in the table are given against normal hydrogen electrode (NHE) as the reference electrode.
[b] Numbers in parentheses denote E values from solution electrochemical studies in Ref. [49].

value, the peak current increases with the sweep rate, thus revealing the diffusion control character of the electrode reaction process, (d) the observed ΔE values (versus NHE) for the cyclic voltammograms decrease as pH increases, and (f) the observed half-wave potentials for **2** and **5** are both lower than the previously suggested value of −800 mV for Ti(IV)–citrate at neutral pH [48]. In this regard, there is ample evidence suggesting that the redox behavior of the species arising as components of the requisite aqueous Ti(IV)–citrate speciation is sensitive to (a) their structural composition and (b) pH. The aforementioned attributes (Table 8) are in concert with the previous observations derived through cyclic voltammetric studies on the binary Ti(IV)–citrate system in aqueous solution [49]. More meticulous work is needed, however, to evaluate the specific behavior of all available pH-structural variants of the binary Ti(IV)–citrate system and establish a detailed relationship of their cyclic voltammetric behavior with the structural composition and pH-sensitivity. Such work is currently ongoing in our labs.

5. Conclusions

Based on the aforementioned grounds, the work, presented herein reflects the significance of structure in defining key physicochemical attributes of components in the aqueous Ti(IV)–citrate speciation [25]. Through careful efforts, a pH-specific "photographic slice" of the distribution profile of aqueous Ti(IV)–citrate systems was extracted, in which the discrete mononuclear species: (a) exhibit a distinct mode of citrate coordination to the Ti(IV) ion in comparison to other octahedrally coordinated congener M(II,III) ions, thereby pinpointing structural attributes that may bear relevance to their respective aqueous chemistries, (b) differ in the degree of deprotonation of the metal-bound citrate ligands, thus projecting structural diversity of the species present in that system's aqueous distributions and the associated complexity, (c) support their participation in the requisite speciation, and (d) display a pH-sensitive association of their structural composition with the redox behavior, as participating structural components of the binary system. Potentially, more diverse Ti(IV)–citrate species should exist in aqueous media that could be isolated and physicochemically characterized. To this end, discrete and well-defined Ti(IV) species, should be in a position to contribute to the delineation of complex ternary interactions of Ti(IV) with (low and high molecular mass) biologically relevant substrates. Such Ti(IV)-assisted ternary interactions may bear relevance and/or association with thus far ill-understood processes involving this metal ion in biological fluids. Logically, then, the aqueous chemistry leading to new characterizable forms of soluble and bioavailable Ti(IV)-hydroxycarboxylate substrates in aqueous media stands imperative, providing an in-depth assessment of physicochemical parameters into that metal ion's potential biochemical behavior. Studies along this direction are currently ongoing in our labs.

Acknowledgements

This research project was supported by a "Pythagoras" grant from the National Ministry of Education and Religious Affairs and a grant co-financed by the E.U. – European Social Fund (75%) and the Greek Ministry of Development – GSRT (25%), Greece.

Appendix A. Supplementary material

CCDC 655393, 655394 and 655395 contain the supplementary crystallographic data for **1**, **2** and **3**. These data can be obtained free of charge from The Cambridge Crystallographic Data Centre via www.ccdc.cam.ac.uk/data_request/cif. Supplementary data associated with this article can be found, in the online version, at doi:10.1016/j.ica.2007.11.015.

References

[1] V. Biehl, T. Wack, S. Winter, U.T. Seyfert, J. Breme, Biomol. Eng. 19 (2002) 97.
[2] R. Thull, Biomol. Eng. 19 (2002) 43.
[3] J. Paladino, D. Stimac, K. Rotim, N. Pirker, A. Stimac, Minim. Invas. Neurosur. 43 (2000) 72.
[4] Y. Sumi, H. Hattori, K. Hayashi, M. Ueda, J. Endodont. 23 (1997) 21.
[5] Y. Yuan, X. Li, J. Sun, K. Ding, J. Am. Chem. Soc. 124 (2002) 14866.
[6] S. Kii, K. Maruoka, Chirality 15 (2003) 68.
[7] D. Bardos, In Titanium and Zirconium Alloys in Orthopedic Applications, in: D.E. Altobelli, J.D. Gresser, E.R. Schwartz, D.J. Trantolo, D.L. Wise, M.J. Yaszemski (Eds.), Encyclopedic Handbook of Biomaterials and Bioengineering, Marcel Dekker, Inc., New York, 1995, p. 509.
[8] M. Degidi, G. Petrone, G. Iezzi, A. Piattelli, Clin. Implant. Dent. Relat. Res. 4 (2002) 110.
[9] C. Knabe, F. Klar, R. Fitzner, R.J. Radlanski, U. Gross, Biomaterials 23 (2002) 3235.
[10] H. Shimizu, T. Habu, Y. Takada, K. Watanabe, O. Okuno, T. Okabe, Biomaterials 23 (2002) 2275.
[11] A. Moroni, C. Faldini, M. Rocca, S. Stea, S. Giannini, J. Orthop. Trauma 16 (2002) 257.
[12] M. Oka, J. Orthop. Sci. 6 (2001) 448.
[13] K. Schneider, A. Müller, E. Krahn, W.R. Hagen, H. Wassink, K.-H. Knüttel, Eur. J. Biochem. 230 (1995) 666.
[14] Z. Schwartz, C.H. Lohmann, A.K. Vocke, V.L. Sylvia, D.L. Cochran, D.D. Dean, B.D. Boyan, J. Biomed. Mater. Res. 56 (2001) 417.
[15] H. Takei, D.P. Pioletti, S.Y. Kwon, K.-L.P. Sung, J. Biomed. Mater. Res. 52 (2000) 382.

[16] J.Y. Wang, D.T. Tsukayama, B.H. Wicklund, R.B. Gustilo, J. Biomed. Mater. Res. 32 (1996) 655.
[17] R.B. Martin, Inorg. Biochem. 28 (1986) 181.
[18] J.P. Glusker, Acc. Chem. Res. 13 (1980) 345.
[19] Z.-H. Zhou, Y.-F. Deng, Y.-Q. Jiang, H.-L. Wan, S.-W. Ng, J. Chem. Soc., Dalton Trans. (2003) 2636.
[20] M. Dakanali, E.T. Kefalas, C.P. Raptopoulou, A. Terzis, G. Voyiatzis, I. Kyrikou, T. Mavromoustakos, A. Salifoglou, Inorg. Chem. 42 (2003) 4632.
[21] M. Kakihana, M. Tada, M. Shiro, V. Petrykin, M. Osada, Y. Nakamura, Inorg. Chem. 40 (2001) 891.
[22] G.M. Sheldrick, SHELXS-86: Structure Solving Program, University of Göttingen, Germany, 1986.
[23] G.M. Sheldrick, SHELXL-97: Structure Refinement Program, University of Göttingen, Germany, 1997.
[24] E.T. Kefalas, P. Panagiotidis, C.P. Raptopoulou, A. Terzis, T. Mauromoustakos, A. Salifoglou, Inorg. Chem. 44 (2005) 2596.
[25] J.M. Collins, R. Uppal, C.D. Incarvito, A.M. Valentine, Inorg. Chem. 44 (2005) 3431.
[26] D. Schwarzenbach, K. Girgis, Helv. Chim. Acta 58 (1975) 2391.
[27] G.M.H. Van de Velde, S. Harkema, P.J. Jellings, Inorg. Chim. Acta 11 (1974) 243.
[28] K. Wieghardt, U. Quiltltzsch, J. Weiss, B. Nuber, Inorg. Chem. 19 (1980) 2514.
[29] D. Schwarzenbach, Inorg. Chem. 9 (1970) 2391.
[30] M. Matzapetakis, C.P. Raptopoulou, A. Terzis, A. Lakatos, T. Kiss, A. Salifoglou, Inorg. Chem. 38 (1999) 618.
[31] M. Matzapetakis, C.P. Raptopoulou, A. Tsochos, B. Papefthymiou, N. Moon, A. Salifoglou, J. Am. Chem. Soc. 120 (1998) 13266.
[32] M. Matzapetakis, M. Dakanali, C.P. Raptopoulou, V. Tangoulis, A. Terzis, N. Moon, J. Giapintzakis, A. Salifoglou, J. Biol. Inorg. Chem. 5 (2000) 469.
[33] M. Matzapetakis, N. Karligiano, A. Bino, M. Dakanali, C.P. Raptopoulou, V. Tangoulis, A. Terzis, J. Giapintzakis, A. Salifoglou, Inorg. Chem. 39 (2000) 4044.
[34] M. Matzapetakis, M. Kourgiantakis, M. Dakanali, C.P. Raptopoulou, A. Terzis, A. Lakatos, T. Kiss, I. Banyai, L. Iordanidis, T. Mavromoustakos, A. Salifoglou, Inorg. Chem. 40 (2001) 1734.
[35] G.B. Deacon, R. Philips, J. Coord. Chem. Rev. 33 (1980) 227.
[36] K. Nakamoto, In Infrared and Raman Spectra of Inorganic and Coordination Compounds Part B, fifth ed., John Wiley and Sons, Inc., New York, 1997.
[37] W.P. Griffith, T.D. Wickins, J. Chem. Soc. A (1968) 397.
[38] N. Vuletic, C. Djordjevic, J. Chem. Soc., Dalton Trans. (1973) 1137.
[39] P.J. Barrie, M. Djuran, M.A. Mazid, M. McPartlin, P.J. Sadler, I.J. Scowen, H. Sun, J. Chem. Soc., Dalton Trans. (1996) 2417.
[40] Y.-F. Deng, Y.-Q. Jiang, Q.-M. Hong, Z.-H. Zhou, Polyhedron 26 (2007) 1561.
[41] J.G. Bledsoe, S.M. Slack, J. Biomater. Sci. Polym. Ed. 9 (1998) 1305.
[42] S.R. Frenkel, J. Simon, H. Alexander, M. Dennis, J.L. Ricci, J. Biomed. Mater. Res. 63 (2002) 706.
[43] C. Vermes, K.A. Roebuck, R. Chandrasekaran, J.G. Dobai, J.J. Jacobs, T.T. Glant, J. Bone Miner. Res. 15 (2000) 1756.
[44] P.L. Palmbos, M.J. Sytsma, D.H. DeHeer, J.D. Bonnema, J. Orthop. Res. 20 (2002) 483.
[45] A. Kapanen, A. Kinnunen, J. Ryhanen, J. Tuukkanen, Biomaterials 23 (2002) 3341.
[46] S.Y. Kwon, T. Lin, H. Takei, Q. Ma, D.J. Wood, D. O'Connor, K.L. Sung, Biorheology 38 (2001) 161.
[47] M. Guo, H. Sun, H.J. McArdle, L. Gambling, P.J. Sadler, Biochemistry 29 (2000) 10023.
[48] M.L. Guo, F. Sulc, M.W. Ribbe, P.J. Farmer, B.K. Burgess, J. Am. Chem. Soc. 124 (2002) 12100.
[49] R. Uppal, C.D. Incarvito, K.V. Lakshmi, A.M. Valentine, Inorg. Chem. 45 (2006) 1795.